Microfluid Nanofluid (2008) 5:711–717
DOI 10.1007/s10404-008-0306-4

SHORT COMMUNICATION

Correlations of droplet formation in T-junction microfluidic devices: from squeezing to dripping

J. H. Xu · S. W. Li · J. Tan · G. S. Luo

Received: 26 March 2008 / Accepted: 12 May 2008 / Published online: 30 May 2008

Abstract In this work, we have systematically analyzed the scaling law of droplet formation by cross-flow shear method in T-junction microfluidic devices. The droplet formation mechanisms can be distinguished by the capillary number for the continuous phase (Ca_c), which are the squeezing regime ($Ca_c < 0.002$), dripping regime ($0.01 < Ca_c < 0.3$), and the transient regime ($0.002 < Ca_c < 0.01$). Three corresponding correlations have been suggested in the different range of Ca_c. In the dripping regime, we developed a modified capillary number for the continuous phase (Ca_c') by considering the influence of growing droplet size on the continuous phase flow rate. And the modified model could predict droplet diameter more accurately. In the squeezing regime, the final plug length was contributed by the growth and 'squeeze' stages based on the observation of dynamic break-up process. In the transient regime, we firstly suggested a mathematical model by considering the influences of the above two mechanisms. The correlations should be very useful for the application of controlling droplet size in T-junction microfluidic devices.

Keywords Scaling law · Monodispersed droplet · Cross-flow shear method · Microfluidic device

J. H. Xu (✉) · S. W. Li · J. Tan · G. S. Luo (✉)
The State Key Lab of Chemical Engineering,
Department of Chemical Engineering,
Tsinghua University, Beijing 100084, China
e-mail: xujianhong@tsinghua.edu.cn

G. S. Luo
e-mail: gsluo@tsinghua.edu.cn

1 Introduction

The development of microfluidic systems which allow for the formation of microdrops inside microfluidic devices has received significant attention over the past 10 years (Kobayashi et al. 2001; Sugiura et al. 2004; Cristini and Tan 2004; Thorsen et al. 2001; Xu and Nakajima 2004; Garstecki et al. 2006; Anna et al. 2003; Xu et al. 2006a, b, c). Monodispersed droplets have been generated via a number of methods in microfluidic devices, including geometry-dominated break-up (Kobayashi et al. 2001; Sugiura et al. 2004), cross-flow shear in T-junction microchannel (Thorsen et al. 2001; Xu et al. 2006a, b, c; Garstecki et al. 2006; Cristini and Tan 2004; Husny and Cooper-White 2006), and hydrodynamic flow focusing (Anna et al. 2003; Xu and Nakajima 2004; Zhou et al. 2006). These methods enable formation of dispersions with highly attractive features, particularly the control over the size and narrow distribution of the sizes of individual droplets. With the rapid development of droplet formation techniques in microfluidic devices, several applications for the microfluidic chemical processing based on droplets have been demonstrated, including production of monodispersed microparticles (Nisisako et al. 2004; Xu et al. 2005; Utada et al. 2005; Gong et al. 2007), enhancement of mixing (Song et al. 2003; Cygan et al. 2005), crystallization of proteins (Zheng et al. 2004), synthesis of nanoparticles (Takagi et al. 2004; Yanagishita et al. 2004), and microchemical analysis (Kumemura and Korenaga 2006; Sun et al. 2006).

One of the most frequently used microfluidic geometries to produce monodispersed droplet is a T-junction by using the cross-flow shear method. The cross-flow shear method utilizes shear force, imposed by an immiscible cross-flow fluid at a T-junction, to generate droplets (drops or plugs),

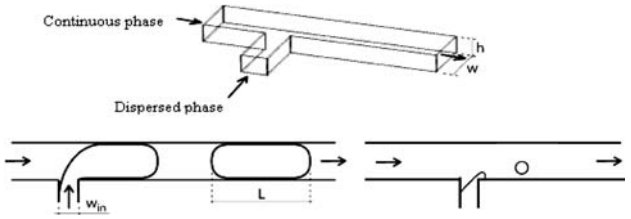

Fig. 1 A schematic illustration of the T-junction microfluidic device (Garstecki et al. 2006)

as shown in Fig. 1. The droplets generated with this method are highly monodispersed with an equal spacing between drops. A lot of work upon droplet formation by cross-flow shear method has been carried out, and the effects of the operational conditions were investigated with different kinds of geometries and working systems. Thorsen et al. (2001) firstly considered droplet formation within a T-junction microchannel. They found that the droplet size decreased with the increase of continuous phase flow rate and continuous phase viscosity in drops flow. They presented a model to predict the droplet size by using the forces balance analyzing of the interfacial force to the viscous force imposed by the continuous phase fluid. Nisisako et al. (2002) and Cristini and Tan (2004) gained similar results in drops flow. While in plugs, flow at low values of capillary number for the continuous phase (herein, $Ca_c = \frac{\mu_c u_c}{\gamma}$, where u_c is the mean flow velocities of the continuous phases, γ the interfacial tension, and μ_c the continuous phases viscosity), the scaling of droplet size was much different. Several groups (Tice et al. 2003; Garstecki et al. 2006; Menech et al. 2008) focused on the scaling law of droplet formation at low values of Ca_c ($Ca_c < 10^{-2}$). They observed experimentally and in numerical simulations (Garstecki et al. 2006; Menech et al. 2008) there was a critical value of capillary number ($Ca_{CR} \sim 10^{-2}$), which distinguished the mechanisms of break-up and the flow regimes of drops flow and plugs flow. When $Ca_c < 10^{-2}$, the interfacial force dominated the cross-flow shear force caused by the continuous phase fluid, and the break-up was determined by the pressure drop across the plug as it formed; when $Ca_c > 10^{-2}$, the cross-flow shear force started to play an important role in the process of break-up, and two-phase flow was in drops flow regime. Then, a quantitative model for the size of plug was suggested by Garstecki et al. (2006) on the basis of dynamic observation and analysis when $Ca_c < 10^{-2}$. The model agreed well with the experimental data in the plugs flow regime. While in the drops flow regime, it was found that (Menech et al. 2008) the droplet formation is strongly affected by the geometry confinement, and the model suggested by Thorsen et al. (2001) is not accurate.

In our previous work (Xu et al. 2006a, b, c), the influences of two-phase flow rate, continuous phase viscosity, and interfacial tension on droplet size were systematically investigated in a T-junction microfluidic device. We also found the different scaling law under different flow patterns. Additionally, the effects of experimental conditions on droplet size in the transient regime were different to that of both the drops flow and plugs flow. So the mechanism of break-up in the transient regime was different.

From the previous review of droplet formation by using cross-flow shear method in T-junction microdevices, the mechanisms of break-up are different in the different regimes. In the squeezing regime, the model suggested by Garstecki et al. (2006) agrees well with the experimental data. In the dripping regime, the model using the forces balance analyzed by Thorsen et al. (2001) and Cristini and Tan (2004) cannot predict the droplet size accurately, and the model should be modified. While in the transient regime, the quantitative model has not been reported yet. So the in-depth understanding of mechanisms of droplet formation in T-junction microchannels is still lacking. In this paper, we attempt to systematically discuss and analyze the scaling of droplet size in different regimes based on our previous experimental work (Xu et al. 2006a, b, c). Firstly, the different two-phase flow patterns (drops flow, plugs flow, and the transient regime) were divided by the capillary number for the continuous phase Ca_c. Then, the corresponding quantitative models were developed based on the analysis of scaling of droplet formation under different range of Ca_c. Finally, we summarized our observations in conclusions.

2 Two-phase flow patterns under different range of Ca_c

From the previous work (Cristini and Tan 2004; Garstecki et al. 2006; Menech et al. 2008), capillary number for the continuous phase is an important parameter to distinguish two-phase flow patterns and the mechanisms of break-up in T-junction microdevices. So we can divide the two-phase flow patterns by Ca_c and discuss the mechanisms of droplet formation in different flow regimes. Herein, we use the experimental data of our previous work (Xu et al. 2006a, b, c). The microdevice in this case has an embedded capillary with a diameter of 40 μm perpendicular to the main channel with 200 μm wide × 150 μm high, which is somewhat different from typical T-junction devices. And we used the embedded capillary as the dispersed fluid channel and continuous fluid channel separately. Figure 2 gives the micrographs of typical droplet formation process. In the experiments, the typical value of two-phase velocity was in the range of 0.001–0.1 m/s, μ_c was in the range of 0.68–10.84 mPa s, and γ in the range of 1.6–3.6 m N/m. So the range of Ca_c was mainly from 10^{-4} to 0.3. It can be seen from Fig. 3 that there are three typical flow regimes

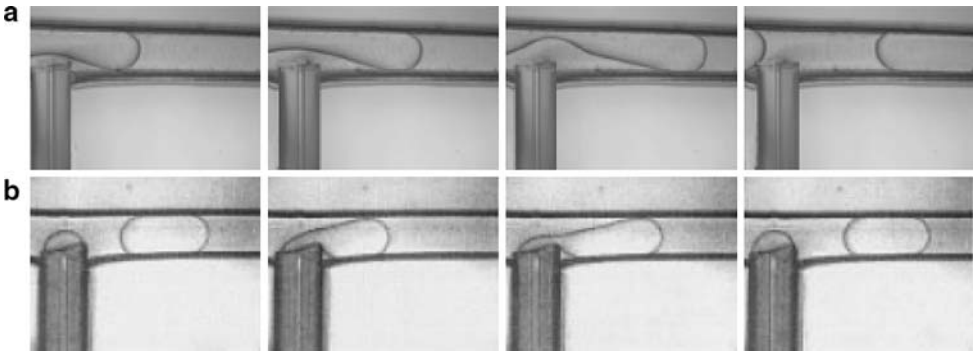

Fig. 2 The micrographs of typical droplet formation process. **a** The capillary was used for supplying the continuous fluid (Xu et al. 2006a, b, c). **b** The capillary was used for supplying the dispersed fluid (Xu et al. 2006a, b, c)

under different values of Ca_c: plugs flow ($l > 2w$, where l is the length of dispersed droplet and w is the width of the channel), drops flow ($l < w$) and the transient regime ($w < l < 2w$). (1) When $10^{-4} < Ca_c < 0.002$, the cross-flow shear force caused by the continuous phase fluid is much lower comparing to the interfacial force and cannot rupture the dispersed phase to drops. So the two-phase flow is in plugs flow regime. In this regime, the interfacial force dominates the shear force, and the dynamics of break-up is dominated by the pressure drop across the plug as it forms, which we call the squeezing regime. (2) When $0.01 < Ca_c < 0.3$, the cross-flow shear force is large enough to play an important role in the process of break-up, and the two-phase flow is in drops flow regime. In this regime, the dynamics of break-up is dominated by the forces balance between shear force and interfacial force, which we call the dripping regime. (3) When $0.002 < Ca_c < 0.01$, the two-phase flow is in the transient regime. In this regime, the dynamics of break-up is dominated by both the earlier two mechanisms. In the following section, we will discuss the scaling of droplet formation under the different range of Ca_c and draw the corresponding models separately.

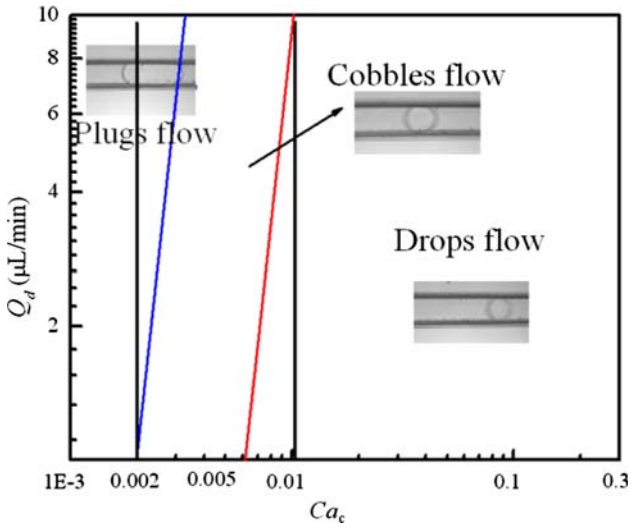

Fig. 3 Two-phase flow patterns under different values of capillary number for the continuous phase Ca_c (Xu et al. 2006a, b, c). The two *oblique lines* to the abscissa are the boundaries between the plugs, cobbles and drops flow. The two *vertical lines* are the boundaries between the squeezing, transient and dripping regimes

3 Driving forces of droplet formation and correlations in different regimes

From the earlier mentioned analysis, there are three regimes that distinguish the mechanisms of droplet formation under the different range of Ca_c.

When $0.01 < Ca_c < 0.3$, the two-phase flow is in the dripping regime. In this regime, the dynamics of break-up is dominated by the forces balance between the shear force and interfacial force

In the previous work (Thorsen et al. 2001; Cristini and Tan 2004), Ca_c was used to represent the balance of cross-flow shear force and Laplace pressure caused by the interfacial tension. So the drops diameter could be described by the equation

$$d_d/d_i \sim 1/Ca_c, \quad (1)$$

where d_i means the cross-section dimension of the microchannel. From Eq. 1 the droplet diameter decreases with the increase of Q_w and continuous phase viscosity μ_c, which is in agreement with the experimental results. Figure 4 shows the comparison between the predicted values and experimental data (Xu et al. 2006a, b, c) under the drops flow patterns. When $Ca_c > 0.2$, they are in good agreement. While $0.01 < Ca_c < 0.2$, the predicted values are rather lager than the experimental results. The main reason for the difference is the influence of droplet size on the continuous phase velocity across the forming droplet when the droplet size is equivalent to the microchannel dimensions. So we modify the capillary number for the continuous phase by considering the effect of droplet size. For a rectangular microchannel with the width w and the height h, the cross-sectional area of a droplet with diameter

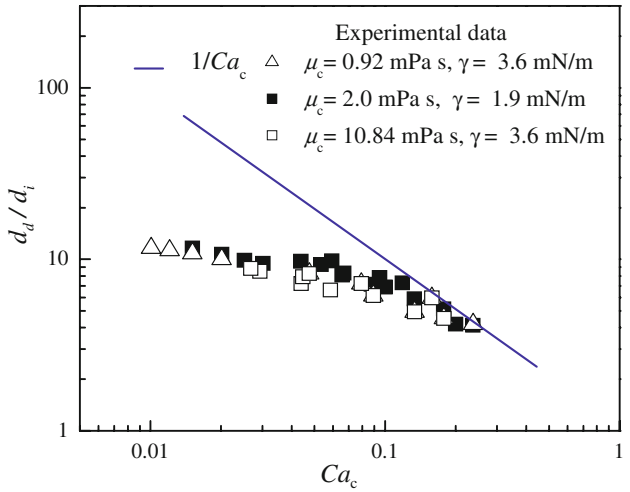

Fig. 4 Comparison of droplet diameter between the predicted values from Eq. 1 and the experimental data from our previous work (Xu et al. 2006a, b, c)

d_{d} is equal to $\frac{\pi}{4}d_{\mathrm{d}}^2 \approx 0.785 d_{\mathrm{d}}^2$, so the modified continuous phase velocity is approximately equal to

$$u_c' = u_c \frac{wh}{wh - 0.785 d_{\mathrm{d}}^2}, \tag{2}$$

where d_{d} is the diameter of the droplet, u_{c} is the average velocity of continuous phase in the channel, $u = Q_c/wh$. So the modified capillary number for the continuous phase $\mathrm{Ca_c}'$ is

$$\mathrm{Ca_c'} = \frac{\mu_{\mathrm{c}} u_{\mathrm{c}}'}{\gamma} = \mathrm{Ca_c} \cdot \frac{wh}{wh - 0.785 d_{\mathrm{d}}^2} \tag{3}$$

From Eqs. (1) and (3),

$$\frac{d_{\mathrm{d}}}{d_{\mathrm{i}}} \approx \frac{1}{\mathrm{Ca_c'}} = \frac{1}{\mathrm{Ca_c}} \cdot \frac{wh - 0.785 d_{\mathrm{d}}^2}{wh}. \tag{4}$$

Equation 4 is the modified model for the droplet size in drops flow when $\mathrm{Ca} > 0.01$. To verify the modified model, we gained the calculated values of droplet diameter from Eq. 4. Figure 5 shows the comparison of droplet diameter between the predicted values and experimental data in the references (Xu et al. 2006a, b, c; Husny and Cooper-White 2006). It can be seen that the modified model predicts the size well for a wide range of $\mathrm{Ca_c}'$ from 0.06 to 0.8 (the value of $\mathrm{Ca_c}$ is from 0.01 to 0.75 correspondingly). For lager values of $\mathrm{Ca_c}$ (when $\mathrm{Ca_c} > 1$), the difference between $\mathrm{Ca_c}$ and $\mathrm{Ca_c}'$ is rather small. So Eq. 4 can be simplified to Eq. 1, which predicted the droplet size very well (Cristini and Tan 2004). From these results, it is necessary to consider the influence of droplet size on cross-flow shear force under the dripping regime, especially when the droplet size is equivalent to the microchannel dimensions.

When $10^{-4} < \mathrm{Ca_c} < 0.002$, the two-phase flow is in the squeezing regime. In this regime, the dynamics of break-up

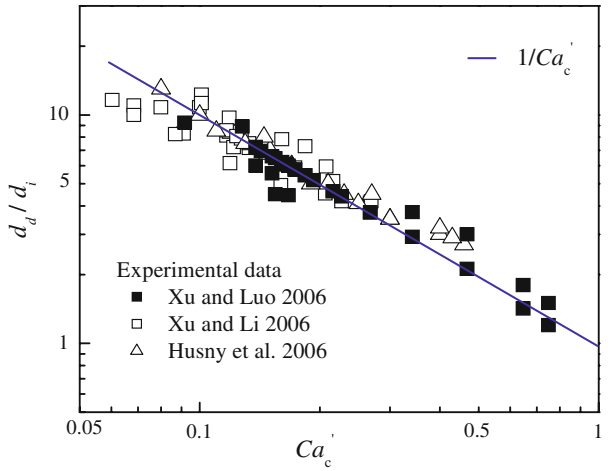

Fig. 5 Comparison of droplet diameter between the predicted values from Eq. 4 and the experimental data from the references. The microdevice in this case has an embedded capillary with diameter of 40 μm for supplying a continuous fluid perpendicular to the main channel (dispersed fluid channel) with 200 μm wide × 150 μm high (*filled square*). The same T-junction microdevices was used, while the main channel was used as the continuous fluid channel and the embedded capillary was used as the dispersed fluid channel (*open square*). A rectangular T-junction microdevice was used in this case. The dimensions of the width in this case were 27.5 and 275 μm for the dispersed phase and the continuous phase, respectively, and the depth was 100 μm (*open triangle*)

is dominated by the pressure drop across the plug as it forms.

On the basis of dynamic observation of break-up process, Garstecki et al. (2006) identified the final length of a plug is contributed by two steps, as shown in Fig. 6. First the tip of the dispersed phase enters and blocks the main channel. At this moment the 'growth length' of the plug is equal to: $L_1 = \varepsilon\, w$, herein ε is a parameter dependent on the geometry of the channel, usually equal to 1. Then the increased pressure in the continuous phase fluid starts to 'squeeze' the neck of dispersed thread. The thickness of the neck (of characteristic width d) decreases at a rate which is approximately equal to the mean speed of the continuous

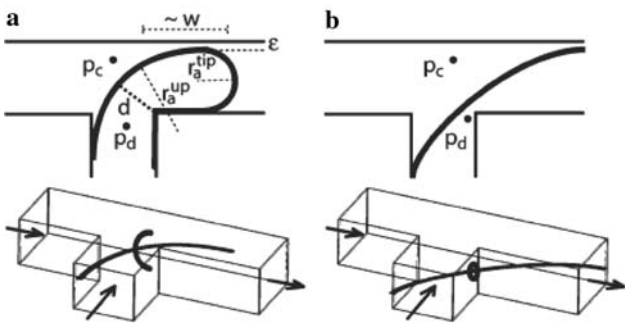

Fig. 6 A schematic illustration of the break-up process of a plug at the junction of the microchannels. **a** the growing stage, **b** the squeeze stage. (Garstecki et al. 2006)

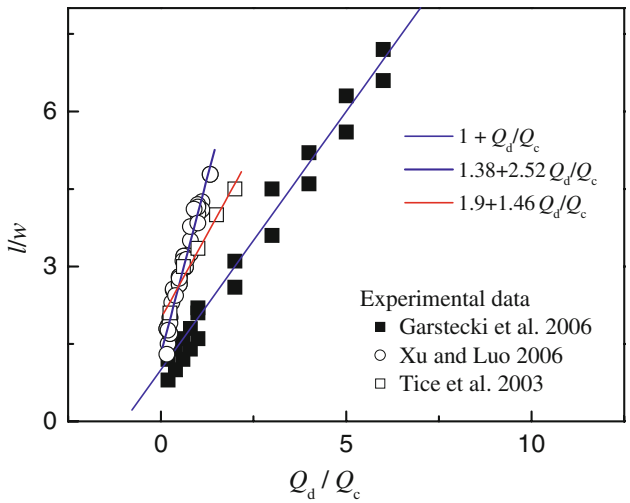

Fig. 7 Comparison of plug length between the fitting results from Eq. 5 and the experimental data from the references. A rectangular T-junction microdevice was used in this case (*filled square*). The dimensions of the width in this case were 50 and 100 μm for the dispersed phase and the continuous phase respectively. The depth was 33 μm. The microdevice in this case has an embedded capillary with diameter of 40 μm for supplying a continuous fluid perpendicular to the main channel (dispersed fluid channel) with 200 μm wide × 150 μm high (*open circle*). A rectangular T-junction microdevice was used in this case (*open square*). The dimensions of the width were both 50 μm for the dispersed phase and the continuous phase

fluid: $u_c = Q_c/hw$. During this process the plug elongates at rate $u_d = Q_d/hw$. So the 'squeeze length' of the plug is $L_2 \approx d/u_c \cdot u_d = d \cdot Q_d/Q_c$. The final length of the plug is therefore equal to $L = L_1 + L_2 = \varepsilon \cdot w + d \cdot Q_d/Q_c$. It is convenient to non-dimensionalize this equation to

$$l/w - \varepsilon = \omega \cdot Q_d/Q_c, \tag{5}$$

where ε and ω are the fitting parameters. The values of ε and ω are mainly affected by the different geometries. We used Eq. 5 to fit the experimental data in the references (Tice et al. 2003; Xu et al. 2006a, b, c; Garstecki et al. 2006). Figure 7 gives the different scaling under the different geometries that have been reported. From these results, the model suggested by Garstecki et al. (2006) can accurately predict the droplet size in the squeezing regime.

When $0.002 < \mathrm{Ca_c} < 0.01$, the two-phase flow is in the transient regime. In this regime, the dynamics of break-up is dominated by both of the mechanisms.

The model describing the scaling of droplet size in this regime has not been reported yet. Considering the two types of influences on the plug length, one is the dynamic break-up of the interface, which could be effected by the two-phase flow ratio Q_d/Q_c mostly; the other is the equilibrium between shear force of the continuous flow and interfacial force, which could be affected by capillary number for the continuous phase $\mathrm{Ca_c}$ mostly. We assume the plug length can be predicted as

$$l/w - \varepsilon = k(Q_d/Q_c)^{\alpha}\left(\frac{1}{\mathrm{Ca_c}}\right)^{\beta} \tag{6}$$

Herein, α and β represent the ratio of the earlier two mechanisms, respectively. There are almost no experiments that discussed the scaling law of plugs size in this regime, except for our previous studies (Xu et al. 2006a, b, c; Tan et al. 2008). So we used Eq. 6 to fit the experimental data in our previous work. The resulted equations are

$$l/w = 0.75\left(\frac{Q_d}{Q_c}\right)^{1/3}\left(\frac{1}{Ca_c}\right)^{1/5} \tag{7}$$

$$l/w = 1.59\left(\frac{Q_d}{Q_c}\right)^{1/5}\left(\frac{1}{\mathrm{Ca_c}}\right)^{1/5} \tag{8}$$

The calculated results from Eqs. (7) and (8) appear to provide a good fit across the whole range of data, as shown in Fig. 8. The differences of exponent between Eqs. (7) and (8) are mainly caused by the different geometries (we used the T-junction and cross-junction geometries separately). From these results, Eq. 6 is relatively accurate in predicting the droplet size in the transient regime.

From the earlier discussion, the break-up of drops/plugs in T-junction microdevices is mainly caused by two different mechanisms: the dynamic break-up of the interface and the equilibrium between cross-flow shear force and interfacial force. There are three regimes which distinguish the mechanisms of droplet formation under the different range of $\mathrm{Ca_c}$. In these regimes, the difference of scaling law is due to the different ratio of the earlier mentioned mechanisms that affect the break-up process. It also shows that the differences of geometries, wetting properties and working systems would cause the different values of parameters in Eqs. (5) and (6). So the models has some limitation, which should be modified for more generality in the forms and the exponents by considering the effects of geometries and the wetting properties in the further work, especially in the transition regime.

4 Conclusions

In this paper, we have systematically analyzed the scaling law of droplet formation by cross-flow shear method in T-junction microfluidic devices. Capillary number for the continuous phase ($\mathrm{Ca_c}$) is an important parameter to distinguish two-phase flow patterns and the mechanisms of break-up. So we divided the two-phase flow patterns by $\mathrm{Ca_c}$ and discussed the correlations of droplet formation in three typical regimes: the dripping, squeezing and transient regimes separately. In the dripping regime, the dynamics of break-up was dominated by the balance between shear force and interfacial force. By considering the influence of

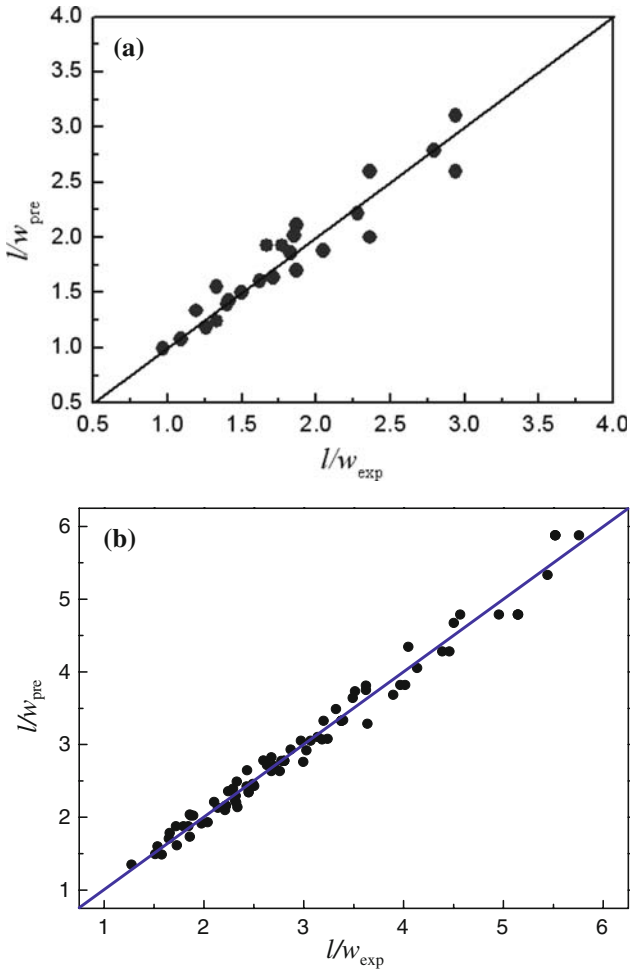

Fig. 8 Comparison of plug length between the fitting results from Eq. 6 and the experimental data from our previous experiments. **a** The T-junction microdevice (Xu et al. 2006a, b, c). **b** The cross-junction microdevice (Tan et al. 2008)

the droplet size on the continuous phase flow rate, we developed a modified parameter of capillary number (Ca_c') by using the local continuous phase flow rate at the droplet formation site. And the modified model could predict droplet diameter more accurately. In the squeezing regime, the dynamics of break-up was dominated by the pressure drop across the plug as it formed. According to the previous work (Garstecki et al. 2006), a mathematical model was suggested to predict the plug length. And the calculated values were in good agreement with the experimental data. In the transient regime, the dynamics of break-up was dominated by the two mechanisms mentioned earlier. Considering the two types of influences on the plug length, we firstly suggested a mathematical model which could predict the plug length accurately. The correlations presented in this work should be useful for in-depth understanding of the mechanisms of break-up by cross-flow shear method and the precise preparation of monodispersed droplets in T-junction microfluidic devices.

Acknowledgments We would like to gratefully acknowledge the supports of the National Natural Science Foundation of China (20490200, 20525622) and National Basic Research Program of China (2007CB714302) on this work.

References

Anna SL, Bontoux N, Stone HA (2003) Formation of dispersions using ''flow focusing'' in microchannels. Appl Phys Lett 82:364–366

Cristini V, Tan YC (2004) Theory and numerical simulation of droplet dynamics in complex flows–a review. Lab Chip 4:257–264

Cygan ZT, Cabral JT, Beers KL, Amis EJ (2005) Microfluidic platform for the generation of organic-phase microreactors. Langmuir 21:3629–3634

Garstecki P, Fuerstman MJ, Stonec HA, Whitesides GM (2006) Formation of droplets and bubbles in a microfluidic T-junction—scaling and mechanism of break-up. Lab Chip 6:437–446

Gong TY, Shen JY, Hu ZB, Marquez M, Cheng Z (2007) Nucleation rate measurement of colloidal crystallization using microfluidic emulsion droplets. Langmuir 23:2919–2923

Husny J, Cooper-White JJ (2006) The effect of elasticity on drop creation in T-shaped microchannels. J Non-Newtonian Fluid Mech 137:121–136

Kobayashi I, Nakajima M, Chun K, Kikuchi Y, Fujita H (2001) Silicon array of elongated through-holes for monodisperse emulsion droplets. AIChE J 48:1639–1644

Kumemura M, Korenaga T (2006) Quantitative extraction using flowing nano-liter droplet in microfluidic system. Anal Chim Acta 558:75–79

Menech MD, Garstecki P, Jousse F, Stone HA (2008) Transition from squeezing to dripping in a microfluidic T-shaped junction. J Fluid Mech 595:141–161

Nisisako T, Torii T, Higuchi T (2002) Droplet formation in a microchannel network. Lab Chip 2:24–26

Nisisako T, Torii T, Higuchi T (2004) Novel microreactors for functional polymer beads. Chem Eng J 101:23–29

Song H, Tice JD, Ismagilov RF (2003) A microfluidic system for controlling reaction networks in time. Angew Chem Int Ed 42(7):767–772

Sugiura S, Nakajima M, Seki M (2004) Prediction of droplet diameter for microchannel emulsification: prediction model for complicated microchannel geometries. Ind Eng Chem Res 43:8233–8238

Sun M, Du WB, Fang Q (2006) Microfluidic liquid–liquid extraction system based on stopped-flow technique and liquid core waveguide capillary. Talanta 70:392–396

Takagi M, Maki T, Miyahara M, Mae K (2004) Production of titania nanoparticles by using a new microreactor assembled with same axle dual pipe. Chem Eng J 101:269–273

Tan J, Xu JH, Li SW, Luo GS (2008) Drop dispenser in a cross-junction microfluidic device: scaling and mechanism of break-up. Chem Eng J 136(2–3):306–311

Thorsen T, Roberts R, Arnold F, Quake S (2001) Dynamic pattern formation in a vesicle-generating microfluidic device. Phys Rev Lett 86:4163–4166

Tice JD, Song H, Lyon AD, Ismagilov RF (2003) Formation of droplets and mixing in multiphase microfluidics at low values of the Reynolds and the capillary numbers. Langmuir 19:9127–9133

Utada AS, Lorenceau E, Link DR, Kaplan PD, Stone HA, Weitz DA (2005) Monodisperse double emulsions generated from a microcapillary device. Science 308:537–541

Xu Q, Nakajima M (2004) The generation of highly monodisperse droplets through the breakup of hydrodynamically focused microthread in a microfluidic device. Appl Phys Lett 85:3726–3728

Xu S, Nie Z, Seo M, Lewis P, Kumacheva E, Stone HA, Garstechi P, Weibel DB, Gitlin I, Whitesides GM (2005) Generation of monodisperse particles by using microfluidics: control over size, shape, and composition. Angew Chem Int Ed 44:724–728

Xu JH, Luo GS, Li SW, Chen GG (2006a) Shear force induced monodisperse droplet formation in a microfluidic device by controlling wetting properties. Lab Chip 6:131–136

Xu JH, Li SW, Tan J, Wang YJ, Luo GS (2006b) Preparation of highly monodisperse droplet in a T-junction microfluidic device. AIChE J 52(9):3005–3010

Xu JH, Li SW, Tan J, Wang YJ, Luo GS (2006c) Controllable preparation of monodisperse O/W and W/O emulsions in the same microfluidic device. Langmuir 22(19):7943–7946

Yanagishita T, Tomabechi Y, Nishio K, Masuda H (2004) Preparation of monodisperse SiO_2 nanoparticles by membrane emulsification using ideally ordered anodic porous alumina. Langmuir 20:554–555

Zheng B, Tice JD, Roach LS, Ismagilov RF (2004) A droplet-based, composite PDMS/glass capillary microfluidic system for evaluating protein crystallization conditions by microbatch and vapor-diffusion methods with on-chip X-ray diffraction. Angew Chem Int Ed 43:2508–2511

Zhou C, Yue P, Feng JJ (2006) Formation of simple and compound drops in microfluidic devices. Phys Fluids 18(092105):1–14